K. KUBOK[*], L. LITYŃSKA-DOBRZYŃSKA[*], J. WOJEWODA-BUDKA[*], A. GÓRAL[*], A. DĘBSKI[*]

INVESTIGATION OF STRUCTURES IN AS-CAST ALLOYS FROM THE Mg-Zn-Ca SYSTEM

BADANIE STRUKTURY ODLEWANYCH STOPÓW MAGNEZU Z UKŁADU Mg-Zn-Ca

Alloys of nominal composition Mg-3Zn-xCa (x = 0, 0.2, 0.5, 0.7, 1.0, 1.3) wt.% have been prepared by resistance melting and casting into graphite mould under argon atmosphere. All investigated alloys have revealed α(Mg) dendritic microstructures with intermetallic phases distributed in interdendritic spacing. The Mg_4Zn_7 has been identified as the main phase which coexists with α(Mg) in the Mg-Zn alloy. Calcium addition causes the formation of ternary $Ca_2Mg_6Zn_3$ hexagonal phase, denoted also as $Ca_3Mg_xZn_{15-x}$. The increase of Mg/Zn ratio from 0.59 in Mg-3Zn-0.2Ca wt.% alloy to 2.72 in Mg-3Zn-1.3Ca wt.% alloy in this phase is connected with an increase in the lattice parameters. The microhardness of the Ca containing alloys increases up to 67 HV (for the alloy containing 1.3 wag.% Ca) compared to the 50 HV for Mg-3Zn wt.% alloy.

Keywords: magnesium alloy, Mg-Zn-Ca, $Ca_2Mg_6Zn_3$, microstructure, TEM

Stopy o składach Mg-3Zn-xCa (x = 0, 0.2, 0.5, 0.7, 1.0, 1.3) %wag. topiono w piecu oporowym w atmosferze argonu i odlano do tygla grafitowego. Wszystkie badane stopy posiadają po odlaniu mikrostrukturą dendrytyczną α-Mg, z obecnością faz międzymetalicznych w przestrzeniach międzydendrytycznych. Główną fazą międzymetaliczną w stopie Mg-3Zn (referencyjnym) była faza Mg_4Zn_7. Dodatek Ca powoduje tworzenie się heksagonalnej fazy potrójnej $Ca_2Mg_6Zn_3$, opisywanej również jako $Ca_3Mg_xZn_{15-x}$. Stosunek Mg/Zn w tej fazie zmienia się od wartości 0.59 dla stopu Mg-3Zn-0.2Ca do 2.72 dla stopu Mg-3Zn-1.3Ca, co związane jest ze zwiększaniem się parametrów komórki elementarnej. Obecność Ca w stopie powoduje wzrost mikrotwardości do 67 HV dla stopu zawierającego 1.3 wag.% Ca (w porównaniu do 50 HV dla stopu Mg-3Zn).

1. Introduction

Nowadays, magnesium alloys from the Mg-Zn-Ca system are in a region of interest in terms of biomaterials engineering as well as in industrial application as lightweight structure materials [1]. In particular, magnesium alloys can be used to manufacture biocompatible and bioresorbable temporary orthopedic implants due to their specific corrosion behavior and mechanical properties similar to that of human bone [2, 3]. Especially lower Young's modulus (∼45 GPa) compared to other metallic materials used for implants and the density (1.7-2.0 g/cm³) makes the material interesting from biomedical point of view [2, 3]. Moreover Mg, Ca and Zn are considered as biocompatible elements and can be metabolized in a human body. The biocompatibility of some alloys from Mg-Zn-Ca system has been indicated by Sun *et al*. [4] and Zhang *et al*. [5]. From a metallurgical point of view the Mg-Zn-Ca system shows better precipitation hardening ability compared to Mg-Zn alloys, which causes higher hardness and creep resistance [6, 7]. Furthermore calcium is believed to be a possible grain refiner in the Mg-Zn system and enhances corrosion resistance of magnesium alloys [4, 6].

Bamberg *et al*. [8] have suggested that precipitation of $Ca_2Mg_6Zn_3$ ternary phase is responsible for the age hardening response in alloys from the Mg-Zn-Ca system and the presence of $CaMg_2$ phase is disadvantageous for this process. The effect is still under investigation by many researchers. Langelier *et al*. [9] have recently reported that presence of $CaMg_2$ has no significant influence on hardness increase in the Mg-0.9Zn-2.1Ca wt.% alloy. What is interesting, they have not found ternary $Ca_2Mg_6Zn_3$ phase in the alloy. Oh-ishi *et al*. [10] have studied several alloys composition with 0.5 wt.% Ca and Zn content up to 4.2 wt.%. It has been found that maximum peak hardness occurs for the optimal composition: Mg-0.5Ca-1.6Zn wt.% alloy. $Ca_2Mg_6Zn_3$ has been identified as responsible for the age-hardening process, but hardness of this alloy is not very high.

Recently, the isothermal section of Mg-Zn-Ca phase diagram at 335°C has been constructed by Zhang *et al*. [11, 12] using diffusion couples method. However insufficient number of samples containing less than 1 at.% Ca have been analyzed. Work of Zhang *et al*. [11, 12] has allowed to resolve some inconsistencies regarding crystal structure of $Ca_2Mg_6Zn_3$ phase [10, 13-16] and the notation $Ca_3Mg_xZn_{15-x}$ has been proposed.

Based on the literature review, particular compositions of alloys with possible good age-hardening response and corrosion behavior have been chosen. Moreover these compositions

[*] INSTITUTE OF METALLURGY AND MATERIALS SCIENCE POLISH ACADEMY OF SCIENCES, REYMONTA 25, 30-059 KRAKÓW, POLAND

can help to fulfill the gap in the Mg-Zn-Ca ternary phase diagram. In order to design a successful implant with proper mechanical and corrosion characteristics or lightweight structural material all data connected with microstructure have to be known. Knowledge about types of phases in as-cast alloys from the Mg-Zn-Ca system allows to understand precipitation sequence during age-hardening treatment. Results obtained by different groups of scientist are not consistent, types of existing phases in the chosen area of isothermal section have not been established yet [11, 12]. Therefore the microstructure, chemical composition and crystal structure of phases in selected alloys from the Mg-Zn-Ca system have been systemically investigated in this work.

2. Experimental procedure

Alloys of nominal composition Mg-3Zn-xCa (x=0, 0.2, 0.5, 0.7, 1.0, 1.3) wt.% have been prepared from Zn (99.999%), Ca (99.9%) and Mg (99.9%) under the argon atmosphere. Calcium has been added in a form of master alloy (Mg-33 Ca wt.%). Melt alloys have been kept for 10 min at 750°C to ensure that all alloying elements have dissolved in the melt. Subsequently melt alloys have been poured into the graphite moulds. Nominal chemical compositions and Ca/Zn ratio of the investigated alloys are listed in Table 1. In this paper all composition of the alloys are described in wt.%.

TABLE 1

Nominal chemical composition of as-cast alloys from the Mg-Zn-Ca system

Alloy	Composition (wt. %)			Composition (at. %)			Ca/Zn (at. %)
	Mg	Zn	Ca	Mg	Zn	Ca	
Mg-3Zn	97	3	–	98.86	1.14	–	–
Mg-3Zn-0.2Ca	96.8	3	0.2	98.74	1.14	0.12	0.11
Mg-3Zn-0.5Ca	96.5	3	0.5	98.55	1.14	0.31	0.27
Mg-3Zn-0.7Ca	96.3	3	0.7	98.43	1.14	0.43	0.38
Mg-3Zn-1.0Ca	96.0	3	1.0	98.24	1.14	0.62	0.54
Mg-3Zn-1.3Ca	95.7	3	1.3	98.05	1.14	0.81	0.71

All specimens for scanning electron microscopy (SEM) and X-ray diffractometer (XRD) have been prepared by standard metallographic procedures. FEI ESEM XL30 with energy dispersive X-ray (EDX) has been used to observe the microstructure of all samples. Preliminary examination of phases in the as cast alloys has been done by XRD using Philips PW 1840 X-ray diffractometer with Co K_α radiation ($\lambda = 1.78896$ Å). Detailed studies of distribution and types of phases have been done by transmission electron microscopy (TEM) using Tecnai G2 F20 (200 kV) microscope equipped with high-angle annular dark field scanning transmission electron microscopy detector (HAADF-STEM) and energy dispersive X-ray (EDX) EDAX microanalysis. TEM specimens have been prepared by twinjet electro-polishing (Tenupol-5) using a solution of 10.6 g lithium chloride LiCl, 22 .32 g magnesium perchlorate $Mg(ClO_4)_2$, 1000 ml methanol, and 200 ml 2-butoxy-ethanol at -40°C and 80 V. Afterwards, the oxide

layer have been removed from the specimen surface using Leica EM RES101 Ion Beam Milling System. Hardness measurements have been performed using CSM Instrument with an indenter load of 1 N (102 g) and a loading time of 30s. Ten indentations have been measured for each sample.

3. Results and discussion

Fig. 1 shows the SEM micrographs of as-cast samples from the Mg-Zn-Ca system and the Mg-3Zn reference sample. All alloys have revealed α-Mg dendrites surrounded by the intermetallic phases. Dendritic microstructure, like in Fig. 1a, has been observed by Gao and Nie [17] for the Mg-8Zn wt.% as-cast alloy. Microstructure for Mg-3Zn-0.5Ca alloy (Fig. 1c) is similar to that observed by Bamberg *et al.* [8] for the Mg-1.9Zn-0.3Ca wt.%. However, in their case micropores have been detected. In this study, the appearance of pores has been avoided due to use of the graphite mould. It is clearly visible that microstructure becomes finer and the amount of intermetallic phases located in the interdendritic region increases with increasing Ca content in the alloy. Therefore, Ca is a possible grain refiner for the Mg-Zn system.
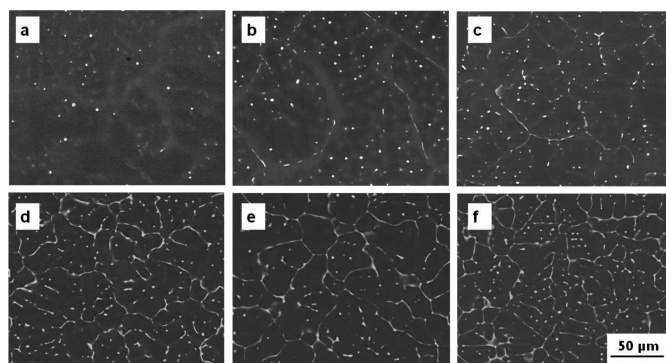

Fig. 1. SEM micrographs of as-cast alloys: (a) Mg-3Zn, (b) Mg-3Zn-0.2Ca, (c) Mg-3Zn-0.5Ca, (d) Mg-3Zn-0.7Ca, (e) Mg-3Zn-1.0Ca, (f) Mg-3Zn-1.3Ca

Fig. 2 shows the XRD spectra of all studied alloys. Except α(Mg), one hexagonal ternary phase $Ca_2Mg_6Zn_3$ has been detected for the alloys containing 0.5 wt.% of Ca or more ($Ca_2Mg_6Zn_3$ phase has hexagonal crystal structure; space group $P6_3$/mmc, with lattice parameters depending on the alloy composition [11]). Reflections of the ternary phase shift towards lower angles with increasing Ca content. It was calculated that the unit cell parameters for the ternary compound change – a: from 9.725 to 9.912 Å, c: from 10.148 to 10.352 Å The same phenomenon has been observed by Zhang *et al.* [11, 12] but for different alloy compositions. New notation $Ca_3Mg_xZn_{15-x}$ has been proposed [11], which seems to be reasonable due to extensive solubility range of this compound. Other phases could not be identified in investigated alloys because of low sensitivity of the method, even $Ca_2Mg_6Zn_3$ phase begins to be detectable in the Mg-3Zn-0.5Ca alloy. Therefore further investigation using transmission electron microscopy has been done.
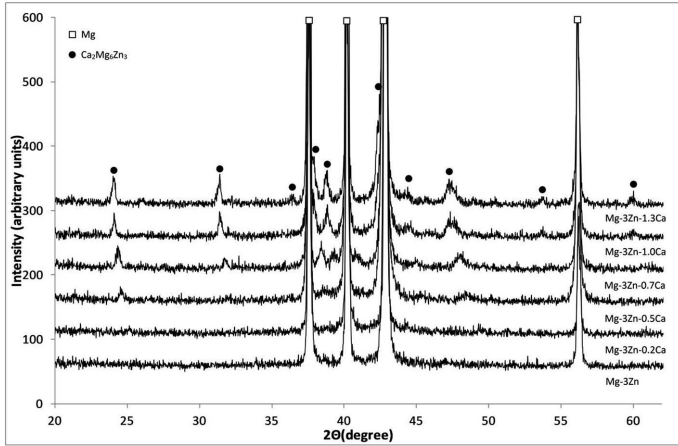
Fig. 2. XRD patterns of investigated alloys from the Mg-Zn-Ca system

Fig. 3a shows STEM-HAADF image of the Mg-3Zn alloy presented particle composed of zinc-rich regions (bright areas) and α-Mg solid solution located between them (dark areas with contrast similar as surrounding matrix). EDX microanalysis has shown that the bright areas contain 35.1 at.% of Mg and 64.9 at.% of Zn, which corresponds to the Mg_4Zn_7 phase. Selected area diffraction pattern (SADP) obtained from the part of Zn rich phase (Fig. 3c) confirms the Mg_4Zn_7 phase (zone axis [101]). The Mg_4Zn_7 phase has a base-centered monoclinic structure (space group C/2m, lattice parameters: a= 25.96 Å, b= c=5.24 Å, c=14.28 Å, β =102.5°) [17]. Bright field TEM image (Fig. 3b) shows that the structure inside the Mg_4Zn_7 particle is not homogeneous and contains high density of planar defects causing streaking of diffraction spots in SADP presented in Fig. 3c. Gao and Nie [17] have identified additionally Mg_7Zn_3 phase formed in interdendritic area in the as-cast Mg-8 wt.% Zn alloy, but this phase has not been observed in this study. It may be caused by different alloy composition or differences in the solidification condition (graphite mould instead pre-heated up to ~200°C steel mould).
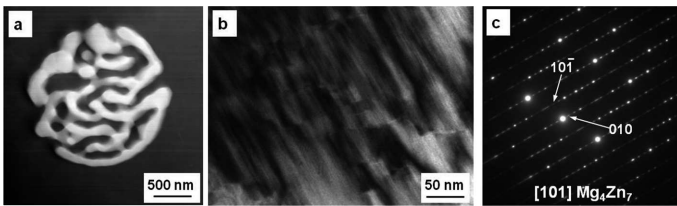

Fig. 3. Mg-3Zn alloy: (a) STEM-HAADF image; (b) TEM bright field image of the magnified part of the particle shown in (a) and (c) corresponding selected area diffraction pattern – [101] zone axis of the Mg_4Zn_7 phase

Apart from the magnesium solid solution, ternary $Ca_2Mg_6Zn_3$ phase is the main intermetallic phase present in calcium containing alloys (detected by XRD for alloys with higher Ca content). This ternary phase coexists with the binary MgZn phase in the Mg-3Zn-0.2Ca alloy. Fig. 4a shows the TEM microstructure of the particle consisting of both phases. This has been confirmed by the results of EDX microanalysis: 51.1 at.% Mg, 46.9 at.% Zn, 2 at.% Ca (MgZn) and 36.6 at.% Mg, 49.6 at.% Zn, 14.2 at.% Ca ($Ca_2Mg_6Zn_3$). Diffraction patterns presented in Fig. 4b and 4c correspond to $Ca_2Mg_6Zn_3$ phase (zone axis [0001]) and MgZn phase (zone axis [$1\bar{2}19$]),

respectively. The MgZn phase has been identified by Khan [18] as a rombohedral crystal structure and expressed in the hexagonal coordinates, with a = 25.69 Å and c = 18.104 Å.
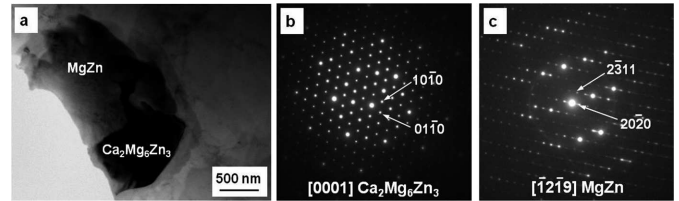

Fig. 4. (a) TEM bright field image of the Mg-3Zn-0.2Ca alloy and (b, c) selected area diffraction patterns for respective phases

For alloys with higher than 0.2 wt.% Ca content only ternary $Ca_2Mg_6Zn_3$ phase coexist with α(Mg) and no trace of $CaMg_2$ binary phase has been found. The binary $CaMg_2$ has been observed by Bamberg et al. [8] and Zhang et al. [11, 12] for similar alloys composition. In Fig. 5 and Fig. 6, exemplary TEM micrographs of the Mg-3Zn-0.5Ca and the Mg-3Zn-1.3Ca alloys are presented, respectively. Figure 5a shows eutectic $Ca_2Mg_6Zn_3$ + α(Mg) located at the grain boundary triple junction, while in the Fig. 5c the interdendritic precipitations of $Ca_2Mg_6Zn_3$ ternary phase are visible. For both cases the $Ca_2Mg_6Zn_3$ phase has been identified by SADPs, taken along [$7\bar{1}89$] zone axis (Fig. 5b) and along [$10\bar{1}1$] zone axis (Fig. 5d). EDX microanalysis results have shown that the compositions of $Ca_2Mg_6Zn_3$ phase are: 57.5 at.% Mg, 29.5 at.% Zn, 13.0 at.% Ca and 54.6 at.% Mg, 33.2 at.% Zn, 12.2 at.% Ca for areas shown in Fig. 5a and Fig. 5c, respectively. In the case of the $Ca_2Mg_6Zn_3$ phase which is the part of eutectic (Fig. 5a), Mg content in $Ca_2Mg_6Zn_3$ phase may be overestimated because of the neighborhood of the α-Mg.
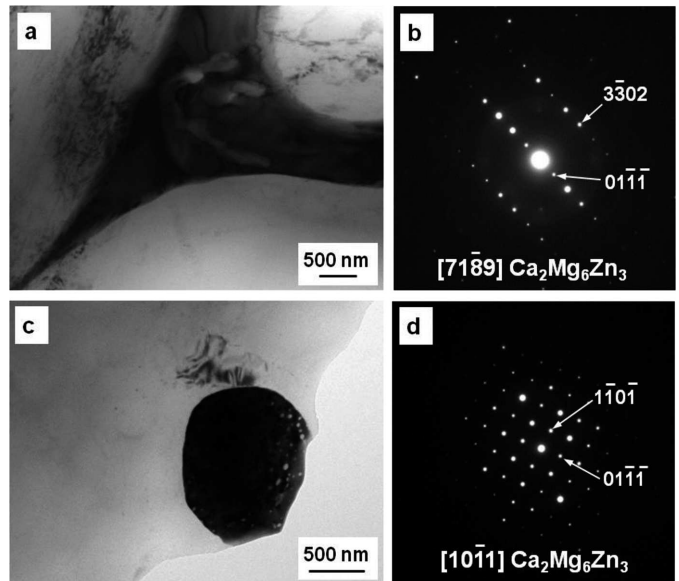

Fig. 5. (a, c) TEM bright field images of the Mg-3Zn-0.5Ca alloy (b, d) corresponding selected area diffraction patterns taken from presented particles

Fig. 6a shows the precipitation of $Ca_2Mg_6Zn_3$ phase in the Mg-3Zn-1.3 alloy. The presence of this phase has been confirmed by SADP taken along [$\bar{1}2\bar{1}0$] zone axis (Fig. 6b).

The composition of this phase in Mg-3Zn-1.3Ca % wt.% alloy is: 60.9 at.% Mg, 26.0 at.% Zn and 13.1 at.% Ca.
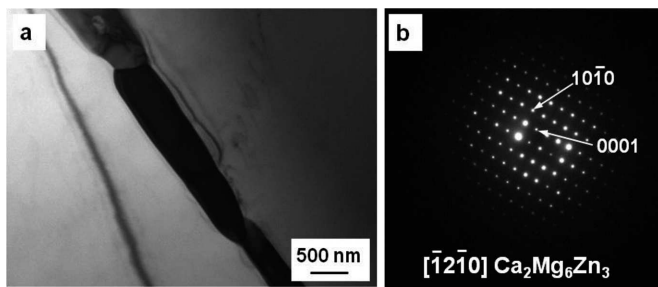

Fig. 6. (a) TEM bright field image of the Mg-3Zn-1.3Ca alloy and (b) corresponding selected area diffraction patterns taken from taken from particle visible in (a)

EDX microanalysis has shown that the composition of the $Ca_2Mg_6Zn_3$ phase is strongly dependent on the composition of the alloy. Therefore several measurements of chemical composition of $Ca_2Mg_6Zn_3$ (for particles lying on the foil edge in order to avoid the influence of the matrix) have been made by EDX. The average value of the obtained results of phase composition, as well as Mg/Zn ratio (in at%) is presented in Table 2. The Mg/Zn ratio in the ternary phase has increased from 0.59 for Mg-3Zn-0.2Ca alloy to 2.72 for Mg-3Zn-1.3Ca alloy, while the Ca content remains at the same level. Similar phenomenon has been recently observed by Zhang *et al.* [11, 12] however in their case the Zn content in alloys has not been fixed. Therefore, due to chosen composition of alloys, it is possible to suggest that addition of Ca to the Mg-Zn system changes the solubility of Zn in Mg. With increasing Ca content in the alloy the atomic fraction of Zn in the ternary phase has been lowered from 54.1 at.% to 22.8 at.%, whereas Mg atomic fraction has increased from 31.8 at.% up to 62.0 at.%.

TABLE 2

Average composition of $Ca_2Mg_6Zn_3$ phase in the investigated alloys

Alloy	Composition (at %)			
	Mg	Zn	Ca	Mg/Zn
Mg-3Zn-0.2Ca	31.8	54.1	14.1	0.59
Mg-3Zn-0.5Ca	51.4	34.5	14.1	1.49
Mg-3Zn-0.7Ca	53.4	31.7	14.8	1.68
Mg-3Zn-1.0Ca	59.7	25.8	14.5	2.31
Mg-3Zn-1.3Ca	62.0	22.8	15.2	2.72

Fig. 7 shows the results of microhardness measurements of as-cast alloys. The microhardness has increased with Ca addition compared to the Mg-3Zn alloy, from about 50 HV to the 67 HV for Mg-3Zn-1.3Ca alloy. The change of microhardness can be explained in relation to the formation of $Ca_2Mg_6Zn_3$ hexagonal phase and the increased amount of this phase with increasing Ca content. However, the increase is not substantial when comparing Mg-3Zn-0.2Ca to Mg-3Zn-1.3Ca alloy. Nevertheless, the change of microhardness is noticeable, what gives high expectation regarding age-hardening of the samples.
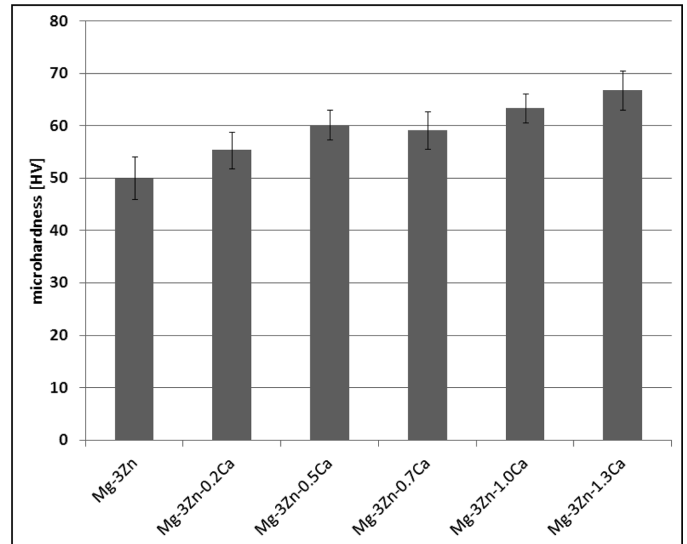

Fig. 7. Average microhardness values with standard deviation bars obtained for investigated alloys

4. Conclusions

1. Six alloys of nominal composition Mg-3Zn-xCa (x = 0, 0.2, 0.5, 0.7, 1.0, 1.3) wt.% have been melt in resistance furnace under protective argon atmosphere using graphite mould.
2. All investigated alloys have revealed α(Mg) dendritic microstructures with intermetallic phases distributed in interdendritic spacing. The Mg_4Zn_7 has been identified as the main intermetallic phase in the Mg-3Zn wt.% alloy. Calcium addition causes the formation of ternary $Ca_2Mg_6Zn_3$ phase. In the Mg-3Zn-0.2Ca wt.% alloy, apart from $Ca_2Mg_6Zn_3$ phase, the MgZn phase has been also identified.
3. Mg/Zn ratio in the $Ca_2Mg_6Zn_3$ phase has increased from 0.59 for Mg-3Zn-0.2Ca wt.% alloy to 2.72 for Mg-3Zn-1.3Ca wt.% alloy. Lattice parameters increase with increasing Ca content (a = 9.725 - 9.912 Å; c = 10.148 - 10.352 Å). It suggests that Ca addition to the Mg-Zn system changes the solubility of Zn in Mg.
4. Microhardness of Ca containing alloys increases to about 67 HV compared to 50 HV for Mg-3Zn wt.% alloy due to the formation of $Ca_2Mg_6Zn_3$.

REFERENCES

[1] S.R. A g n e w, J.F. N i e, Scr. Mater. **63**, 671 (2010).
[2] E. G h a l i, Metallurgically and microbiologically influenced corrosion of magnesium and its alloys, in: E. Ghali(Ed.), John Wiley&Sons Inc. (2010).

[3] X. W a n g, J.S. N y m a n, X. D o n g, H. L e n g, M. R e y e s, Fundamental Biomechanics in Bone Tissue Engineering, in: K.A. Athanasiou and J. Kent Leach(Ed.), Synthesis Lectures on Tissue Engineering, Morgan & Claypool Publishers (2010).

[4] Y. S u n, M. K o n g, X. J i a o, Trans. Nonferrous Met. Soc. China **21**, 252 (2011).

[5] B. Z h a n g, Y. H o u, X. W a n g, Y. W a n g, L. G e n g, Mater. Sci. Eng., C **31** , 1667 (2011).

[6] F. N i e, B.C. M u d d l e, Scr. Mater. **37**, 1475 (1997).

[7] C.J. B e t t l e s, M.A. G i b s o n, K. V e n k a t e s a n, Scr. Mater. **51**, 193 (2004).

[8] M. B a m b e r g e r, G. L e v i, J.B.V. S a n d e, Metall. Mater. Trans. A **37**, 481 (2006).

[9] B. L a n g e l i e r, X. W a n g, S. E s m a e i l i, Mater. Sci. Eng., A **538**, 246 (2012).

[10] K. O h - i s h i, R. W a t a n a b e, C.L. M e n d i s, K. H o n o, Mater. Sci. Eng., A **526**, 177 (2009).

[11] Y. Z h a n g, D. K e v o r k o v, J.L.E. E s s a d i q i, M. M e d r a j, Intermetallics, **18**, 2404 (2010).

[12] Y. Z h a n g, D. K e v o r k o v, F. B r i d i e r, M. M e d r a j, Sci. Technol. Adv. Mater. **12**, (2011).

[13] R. P a r i s, Publications Scientifiques et Techniques du Ministère de L'Air, Ministère de L'Air, **45**, 1 (1934).

[14] J.B. C l a r k, Trans. AIME **221**, 644 (1961).

[15] T.V. L a r i n o v a, W.W. P a r k, B.S. Y o u, Scr. Mater. **45**, 7 (2001).

[16] P.M. J a r d i m, G. S o l o r z a n o, J.B.V. S a n d e, Mircoscopy and Microanaysis **8**, 487 (2002).

[17] X. G a o, J.F. N i e, Scr. Mater. **57**, 655 (2007).

[18] Y. K h a n, J. Mater. Sci. Eng. **24**, 963 (1989).